To appear in: B. Schmieder, A. Hofmann and J. Staude (Eds.), *Solar Magnetic Fields and Oscillations*, Procs. Third Adv. Solar Phys. Euroconf., Astron. Soc. Pac. Conf. Series, 1999.
Preprint via WWW: `http://www.astro.uu.nl/~rutten/`
via ftp: `ftp.phys.uu.nl, cd pub/astronomy/rutten, get potsrev.ps.Z`

(Inter-) Network Structure and Dynamics

Robert J. Rutten

Sterrekundig Instituut, Utrecht, The Netherlands

Abstract. The dynamical nature of the low solar atmosphere outside active regions is emphasized by recent observations and simulations alike. La Palma images, MDI maps, SUMER spectra, TRACE movies, hydrodynamic shock simulations and magnetohydrodynamic sheet simulations all impart non-quiet behavior to the "quiet Sun". This review begins with a brief summary of current insights and then focuses on various quiet-Sun questions that seem pertinent and solvable.

1. Introduction: network and internetwork

Figure 1 overleaf defines the topic of this review. Outside active regions, the remaining "quiet sun" appears sparsely speckled on photospheric magnetograms (left) and chromospheric filtergrams (right). The bright chromospheric speckles overlie patches of positive or negative field concentrations in the photosphere. The speckles and patches are arranged in roughly cellular patterns called the "magnetic network" and "chromospheric network", repectively, or simply "the network" because they coincide closely.

The magnetic/brightness patches make up the "network boundaries". The remaining areas, mostly free of kilogauss field and much darker in Ly α and other chromospheric lines, are called "internetwork". Big Bear authors use "intranetwork" but like "intravenous" that should mean inside the boundaries themselves. From Würzburg and Göttingen comes "cell interior", also a misnomer because the network does a poor job in outlining the supergranulation cells measured in photospheric Dopplershift away from disk center — at low activity it is hard to recognize cell boundaries from the sparse network patches. At larger flux density the network maps the sink sites more completely, but the flows are then upset by the fields. The name "non-network" proposed by Keller et al. (1994) implies everything else, like "non-LTE".

Figures 2–4 constitute a cartoonwise review of (inter-)network properties. They serve here to provide paradigmwise context to the selected issues discussed questionwise below. I review them briefly, bracketwise adding principal paradigmal culprits.

Figure 2 portrays the major actors on the (inter-)network scene. The magnetic network is made up of clusters of kilogauss [Spruit 1977] fluxtubes that

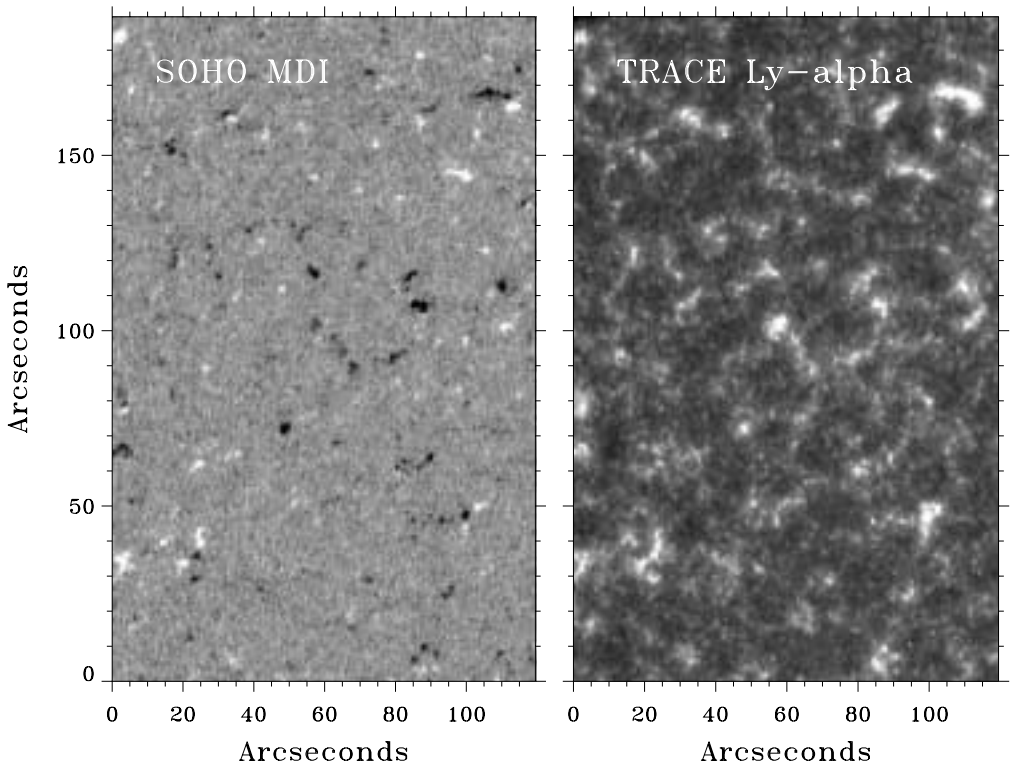

Figure 1. Part of an MDI magnetogram and a co-aligned part of a simultaneous TRACE Ly α filtergram. The chromospheric emission pattern at right corresponds closely with the photospheric magnetic field pattern at left, irrespective of polarity, except for the small-scale background graininess which is dominated by noise at left and by acoustic oscillation patterns at right. Data taken on June 14, 1998, reduced by C.J. Schrijver and H.J. Hagenaar.

used to be observed as [Dunn & Zirker 1973] filigree from Sac Peak (Fig. 5) but are now best seen as chains of [Muller 1994] bright points in the 430.5 nm [Fraunhofer 1817] G band from Pic du Midi and La Palma (Fig. 6), or alternatively as numerical flux sheets in [Steiner et al. 1998] simulations where they are embedded in fast [van Ballegooijen 1985] downflows and occasionally send shocks into the upper atmosphere. Higher up, the fluxtubes in the clusters expand, combine into bundles, flare out into low-lying [Giovanelli 1980] canopies, and either extend openly out harboring the solar wind or bend closedly back harboring coronal loops (Fig. 3). The magnetic heating of the chromospheric network (shaded in Fig. 2) seems concentrated in the bundles since the network remains grainy in [Reeves 1976] ultraviolet images sampling temperatures up to 10^5 K.

The internetwork is free of kilogauss fields except for occasional [Harvey & Martin 1973] ephemeral active regions not shown here. Small transient patches of weak horizontal field occur more ubiquitously (HIF = horizontal internetwork

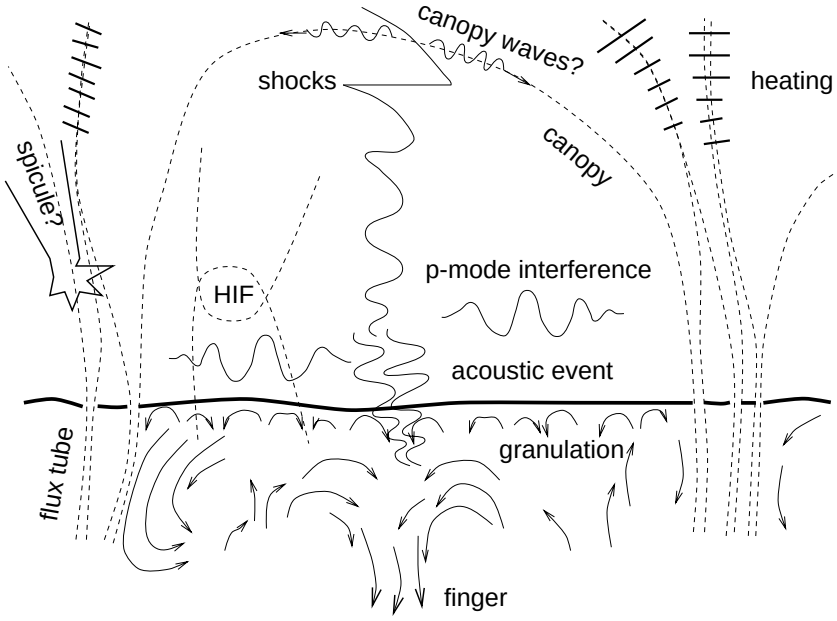

Figure 2. Cartoon of the radial structure of the low solar atmosphere outside active regions, portraying a vertical cut through a photospheric supergranulation cell with magnetic network at and chromospheric network above its cell borders. Dashed: magnetic field. Arrows: convective flows. Thin wavy lines: horizontal/vertical oscillatory velocity. Hatching: magnetodynamical heating. Adapted from Rutten (1998).

field, Lites et al. 1996) and may mark flux emergence (an apparently separating newly appeared dipole) too weak to be seen as an ephemeral region, or cancellation (an apparently contracting and vanishing dipole) too weak to be seen as a [Golub et al. 1974] X-ray bright point, or the horizontal segments of a $\bigcap$ or $\bigcup$ surface-breaking undulation of a weak Omega loop or a [Spruit et al. 1987] sea serpent.

The non-magnetic shallow granulation pancake pattern is caused by radiative losses from convective upwellings. The photons escape suddenly from their adiabatic confinement — close enough to favor convective energy diffusion and to make them obey the local temperature as if they were sluggish fermions — all the way out to probe the far depths of the universe. Their abrupt departure leaves [Stein & Nordlund 1989] downflow fingers driving large-granule fragmentation (Rast 1995) and kills small granules with accompanying collapse blasts ("acoustic events") that may dominate global p-mode excitation (Goode et al. 1998, Rast 1999a, 1999b) and the production of acoustic shocks in the overlying chromosphere (Hoekzema & Rutten 1998, Hoekzema et al. 1998a, Skartlien 1998). The latter shocks explain the Ca II H_{2V} and K_{2V} grains (Rutten & Uitenbroek 1991, Carlsson & Stein 1994, 1997, Rutten 1995), disavow (Carlsson & Stein 1995) standard modeling of the solar chromosphere, partially reflect fresh upcoming waves into standing resonances (Carlsson & Stein 1999, these proceedings), and may excite small-scale canopy waves (Hoekzema et al. 1997).

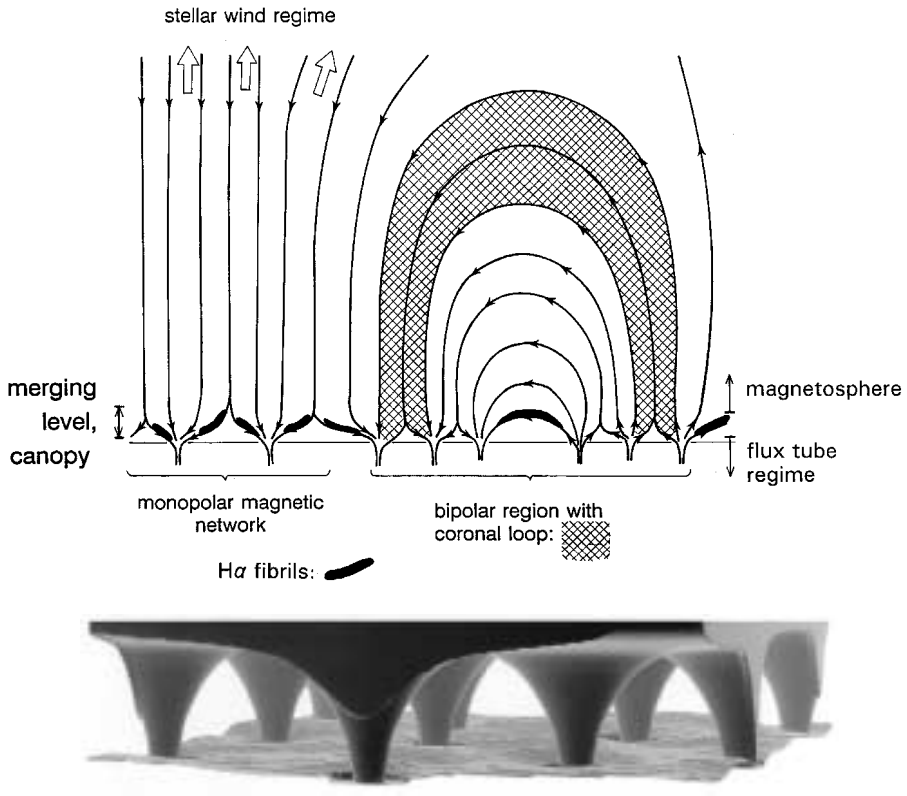

Figure 3. Magnetic field topology according to K&K (Schrijver & Zwaan 1999). The lower part illustrates fluxtube spreading for monopolar network. The upper part sketches a vertical cross-section including higher layers, split between open-field solar wind regime emanating from monopolar network and closed-field regime with a coronal loop extending from bipolar footpoints. Hα fibrils outline low-lying field lines.

Figure 3 extends the radial cut of Fig. 2 to larger height (upper part) and into horizontal perspective (lower part). It is taken from an upcoming book by C.J. Schrijver and C. Zwaan called "Solar and Stellar Magnetic Activity" and abbreviated K&K henceforth. The lower part schematizes fluxtube spreading and merging in a 3D rendering of the Zürich wine glass model of Bünte et al. (1993). The upper part came from Zwaan & Cram (1989) and schematizes open and closed field topology in the corona, with Hα fibrils outlining the inclined lower parts and coronal loops outlining the closed upper parts.

Figure 4 illustrates network topology on yet larger scale. This is the "magnetic carpet" of NASA press-release fame based on MDI magnetometry. It symbolizes the dynamical balance in quiet-sun network maintenance between flux gains and losses and the corresponding dynamical reconfiguring of the overlying coronal field connections (Schrijver et al. 1997). The gains are better established than the losses. About one ephemeral region emerges per supergranule per day as a small 10^{19} Mx dipole, followed by rapid unfolding in which the footpoints

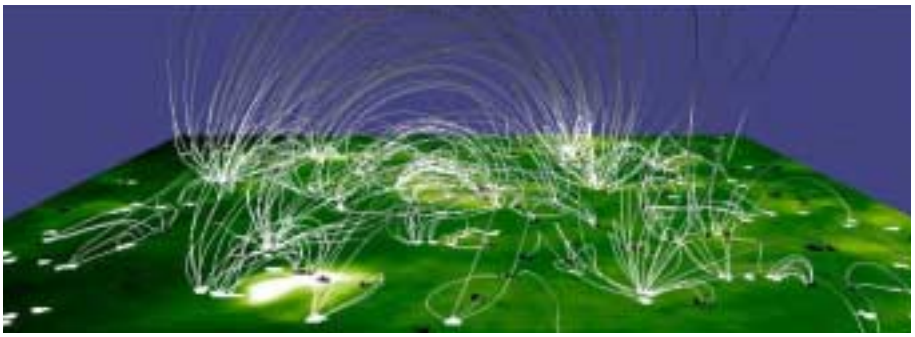

Figure 4. The solar magnetic carpet according to Schrijver et al. (1998). Long and short coronal loops connect network patches. The dynamical topology changes of the latter, balancing flux input from ephemeral regions against flux disappearance, enforce continual reconfiguration and reconnection of the fields higher up. Figure by C.J. Schrijver and N.E. Hurlburt, copied from `http://www.lmsal.com/magnetic.htm`.

separate over 5–10 arcseconds and by slower subsequent footpoint migration, at local flow speeds and taking a few hours, to the network to which they add flux if the polarities fit and otherwise "cancel" against reverse polarity features (flux vanishing from a bipolar pair until the weakest is gone, Livi et al. 1985, Martin 1988; see also Wang & Zhang 1999 in these proceedings). The losses should be incurred through field reconnection, shredding, subduction, or uplift. The current balance estimate says that all bipolar quiet-sun network is reprocessed every forty hours. Monopolar network, left over from a previous active region, does not loose its polarity excess when sweeping up bipolar ephemeral regions and keeps its sign signature much longer.

2. Network issues

Facular points or network bright points or filigree grains?
Fluxtubes or flux bundles or magnetic elements?

These questions are similar even though observational and theoretical, respectively. What are the basic network elements and what should we call them? Figure 5 is a classic Hα filigree picture from Sac Peak. Yet better ones were taken in the Mg I b_1 wing by Beckers (1976; also displayed as frontispiece in *Solar Phys.* 43, 271 and on page 268 of Foukal 1990) and have been analysed in detail by Spruit & Zwaan (1981). Nowadays, the network elements are observed most often and most brightly in the molecular CH band around $\lambda = 4305\,\text{Å}$ called G by Fraunhofer, from Pic du Midi and La Palma (e.g., Muller et al. 1989, 1999, Auffret & Muller 1991, Muller & Roudier 1992, Roudier et al. 1994, Berger et al. 1995, 1998, Berger & Title 1996, Title & Berger 1996, Löfdahl et al. 1998). Figure 6 shows an example. Mehltretter called them "facular points", Muller calls them "Network Bright Points" after Stenflo & Harvey (1985), I have called them "Muller bright points", Berger et al. (1998a) call them "magnetic

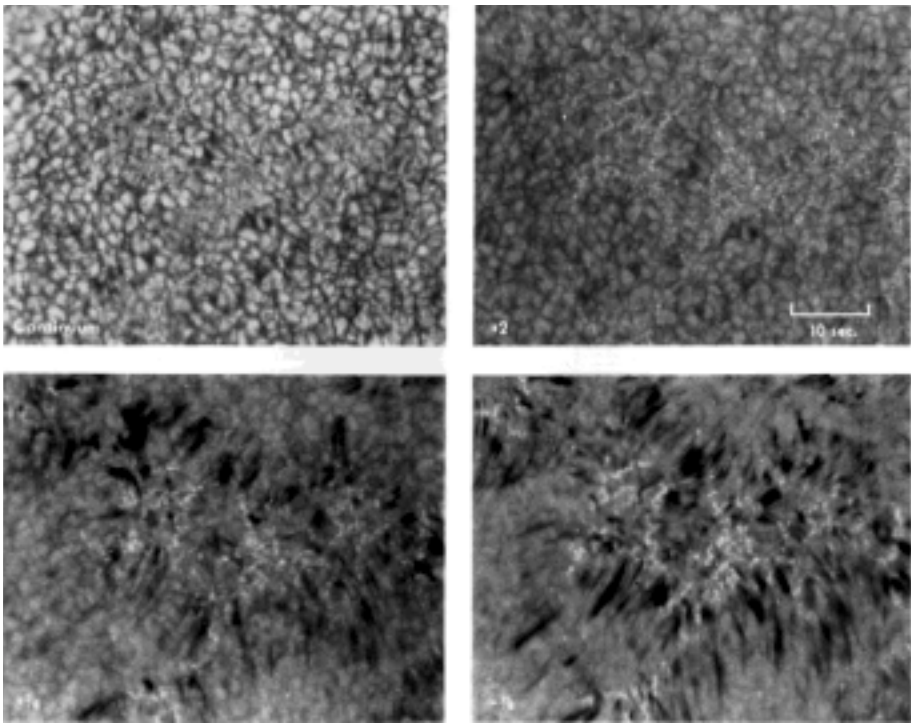

Figure 5. Solar filigree on filtergrams taken with a Zeiss tunable Hα filter at the Dunn Solar Telescope by Dunn & Zirker (1973). The presence of small-scale magnetic elements is evident by their disruption of convection patterns in the continuum (abnormal granulation, upper left panel) and as bright grain clusters in the Hα wings at $\Delta\lambda = +2, +7/8, -7/8$ Å. Also reproduced on page 268 of Stix (1989) and in many other books. From `http://vtt.sunspot.noao.edu/gifs/fill1.gif`.

bright points", K&K call them "filigree grains". The last name seems the more appropriate one since it properly credits Dunn & Zirker (1973), indicates that the little features often appear as beads in a string, and expresses their size as small but yet extended (perhaps elongated) whereas "point" implies infinitesimal smallness.

The second panel of Fig. 6 shows the same area in Ca II K, i.e., low-chromosphere brightness. (The TRACE near-UV channels would show much the same, cf. Rutten et al. 1999.) Comparison with the G-band panel at left shows immediately that most emission patches of the chromospheric network overlie *clusters* of filigree grains. The paradigm of fluxtube expansion into canopy, whether compared to wine glasses in Zürich or to gothic vaults as in Fig. 3, should therefore be replaced by fluxtube *bundles* combining higher up — as sketched in Figs. 2 and 8.

Playing sequences of such G-band images as movies shows dramatically that the filigree grains come and go in highly dynamical fashion. They are bumped around by granules, split up, recombine, become bright and vanish from

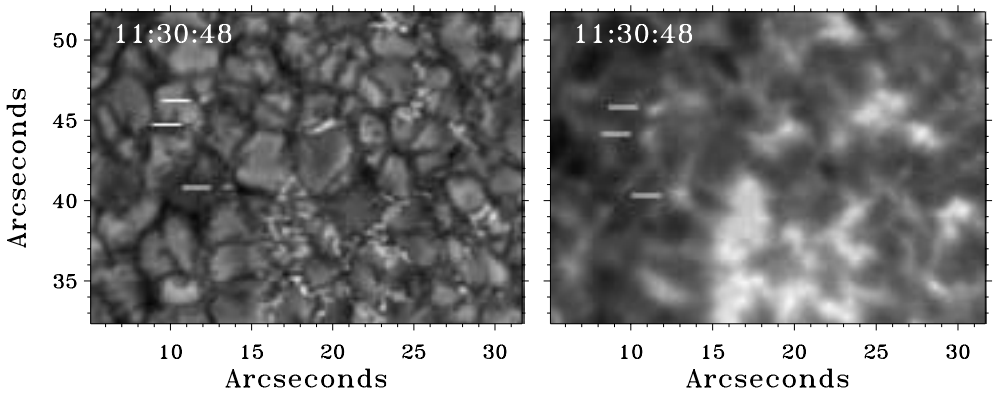

Figure 6. Left: part of a high-resolution (0.2 arcsec) G-band filtergram (bandpass 10 Å FWHM) from a sequence taken by R.A. Shine with the Swedish Vacuum Solar Telescope at La Palma, restored using phase-diverse speckle sampling by Löfdahl et al. (1998) and analyzed by Berger et al. (1998a, 1998b). Right: simultaneous Ca II K filtergram (bandpass 3 Å FWHM) of the same area, non-restored. The diffuse patches of Ca II K network emission overlie clusters of tiny filigree grains. The three marked isolated features might be classified as K_{2V} internetwork grains ("cell flashes") in a single Ca II K image such as this one, but when the two image sequences are displayed as movies these features are seen to represent "persistent flashers" that show up intermittently, tracking the disappearing and reappearing filigree grains underneath. From Lites et al. (1999).

sight within minutes even though magnetism remains detectable on simultaneous magnetograms (Muller et al. 1999, these proceedings). Probably the fluxtubes do not produce filigree grains all the time; Berger et al. (1998a) found that "magnetic bright points" represent "magnetic elements" but incompletely, an old issue initiated by Simon & Zirker (1974) to which I return in Fig. 8.

Why are filigree grains so bright in the G band?

Filigree grains tend to be bright in the continuum at sufficient resolution; at lower (but yet subarcsecond) resolution they vanish due to smearing with the darkness of the surrounding intergranular lane (Title & Berger 1996). The cospatial G-band and continuum images of Löfdahl et al. (1998) show that the G-band shows the same filigree grains as the continuum but much brighter. Why?

Conventional wisdom says that filigree grains brighten in the G band because the CH lines cause radiation escape somewhat higher up in the atmosphere where the fluxtubes are already heated. Wrong on both counts, I think. First, G-band images display granules much the same as any nearby wide-band continuum, instead of the reversed contrast they should show when portraying the middle photosphere. Second, bright doesn't necessarily mean locally hot.

My answer to this question is cartoonized in Figs. 7–8. Two properties make the CH lines special: the low CH dissociation energy (only 3.5 eV from

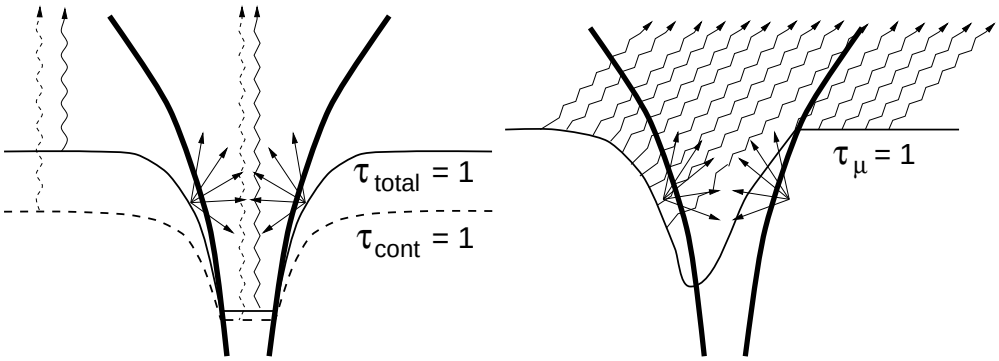

Figure 7. Formation of filigree grains in the G band from an idealized fluxtube. Left: the hot tube walls (thick curves) irradiate the tube inside so that the CH molecules there photodissociate and the line opacity in the G band diminishes. The representative $\tau_{\rm total} = 1$ photon escape depth at disk center therefore has a much larger Wilson depression than it would have for the line-free continuum alone (dashed). Right: photons that escape slantedly (here at 45 degrees and observed from apparent radius $r/R_\odot = 0.707$) sample the radial temperature gradient outside the tube at $\tau_\mu = 1$ along the rays as a slightly extended bright stalk. Comparable photoionization affects the far wings of Hα and the Mg I b lines to produce similar filigree grains.

the ground state, even lower than K I with its 4.3 ev), and the curtailing of CH formation at heights where CO associates (Mount 1975). The first makes CH particularly sensitive to photodissociation by near-UV photons. In the fluxtube paradigm depicted in Fig. 7, CH gets split by hot-wall irradiation within the tube. The resulting absence of line opacity inside the tube produces a much larger Wilson depression, with attendant Spruit (1976) contrast enhancement, than in the pure continuum or in a wavelength band with atomic lines that are less susceptible to photoionization.

The outer wings of Hα have similar opacity sensitivity to near-UV irradiation because the lower level is only 3.4 eV from the H I continuum and discoupled from the LTE ground state population. The Mg I b triplet is also particularly sensitive to irradiative splitting because its lower $3p\ ^1{\rm P}^o$ level (5.0 eV from the Mg I ionization limit) provides the main channel for photoionization closure in a loop driven by infrared photon suction (Fig. 12 of Carlsson et al. 1992, explanation for both H I and Mg I in Rutten & Carlsson 1994). In each case the line opacity and the enhancing effect of its depletion peak in deep layers, for CH because it is cut off by CO formation higher up and for the Hα and Mg I b wings because the damping wing opacity diminishes at lower collider density.

Thus, my conjecture is that the bright filigree grains are formed deep and that they do not represent material heating within the tube. Towards the limb, they should show up as little bright stalks. Obviously, it takes multidimensional fluxtube simulation with detailed ionization/dissociation balance modeling to compute filigree grains properly. One-dimensional fluxtube modeling based on Fe I or Mg I b line polarimetry may have underestimated ionization and therefore

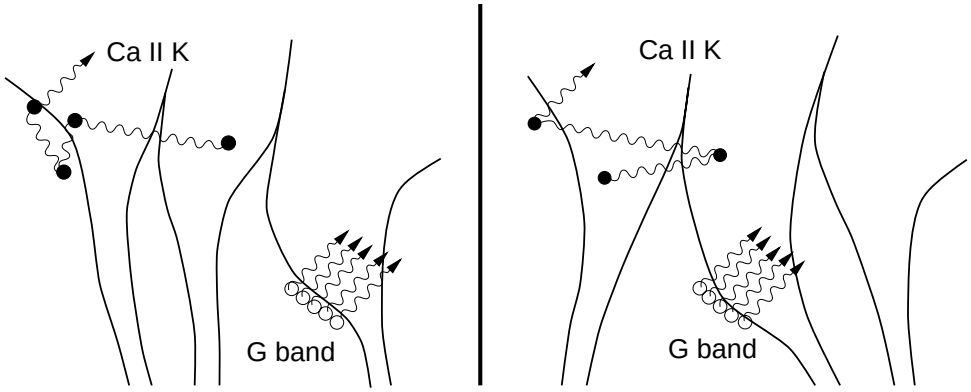

Figure 8. Formation of filigree grains and chromospheric network grains from more realistic magnetic elements than the fluxtube of Fig. 7. Vertical cross-sections at two instants a few minutes apart. Open circles: recombining photospheric H^- ions. Solid circles: chromospheric Ca II ions. Three magnetic elements make up a close-spaced row in an intergranular lane. Their lower parts are pushed aside over small distances by a neighboring granule (not shown) while the collective flux bundle higher up remains stable. Left: a bright filigree grain occurs because a hot wall segment creates G-band photons by H^- recombination and sends them off to the observer through the CH-free opacity void that results from local irradiation. A Ca II K photon is created higher up in a flux concentration but then scatters a few times off other calcium ions before it escapes towards the observer. Both the G-band and the Ca II K radiation sample creation temperature, but the Ca II K ray does not do so for the location from which it appears to come. Right: the same trio produces a different G-band filigree grain a few minutes later but appears about the same in Ca II K.

overestimated line formation temperature by not including such transverse hot-wall irradiation.

Why are filigree grains so sharp?
How well do filigree grains map fluxtubes?

Two related questions that are possibly answered by Fig. 8. Magnetic elements in the 2D Freiburg simulations (see Steiner's review in these proceedings) are already very dynamic, being subject to pushy convective flows on their sides, but actual magnetic elements should be even more dynamic from 3D instabilities. Filigree grain formation may therefore vary markedly with time, depending on the instantaneous fluxtube geometry. The G band and the Mg I b and Hα wings may show us rather small patches of bright wall, as sketched in Fig. 8. These diagnostics have LTE source function response since the H^- bound-free continuum dominates the photon production with $S_{\rm cont} = B_\nu(T)$. For the G band the remaining bound-bound photon production also has $S_{\rm line} \approx B_\nu(T)$ with the relevant CH population ratios obeying local Boltzmann ratios even while the CH dissociation balance and line extinction are non-locally upset. Thus, filigree

grain brightness should faithfully portray the temperature at $\tau_\mu \approx 1$ along each line of sight. That makes filigree grains already sharp. Figure 8 suggests that they may be even sharper and faster-varying than the magnetic elements whose presence they betray.

Why are the network grains less sharp?

Figure 8 also adds the chromosphere and the formation of Ca II K photons that produce a network grain on Ca II K filtergrams. These photons scatter over appreciable distances, up to 500-1000 km (about five local scale heights) before they finally escape. Their creation location and temperature may differ substantially from where we see them come from. In addition, the steep variation of line extinction over the Doppler core, typically four orders of magnitude, produces appreciable mixing of representative $\tau = 1$ escape depths even in narrowband Ca II K filtergrams. Also, the scattering is partially coherent and partially Doppler-redistributed, yet another fuzzying complication.

Thus, even if fluxtubes were narrow, ramrod straight, and obeyed the same temperature gradient as the surrounding atmosphere, scattering would produce hazy chromospheric emission patches (cf. Kneer 1981). It isn't therefore clear whether the fuzziness of the network grains in the Ca II K panel of Fig. 6 comes from merging as sketched in Fig. 8 or from scattering; probably from both. The same holds for the G to K size increase of the three isolated features marked in Fig. 6. Solanki et al. (1991) supported their 1.5D transfer modeling along rays with the argument that wine-glass fluxtubes flare out to widths of 2000 km, wider than the scattering paths where the latter become large. The trio sketched in Fig. 8 covers smaller width than the scattering paths. The radiative transfer nut to crack is a harder one than for the filigree grains. In NLTE terms it is the reverse because multidimensional non-locality affects the source function in this case while there is no ionization balance = opacity problem, Ca II being the dominant stage everywhere. Solving the scattering problem requires establishing the nature and role of nonthermal broadening in partial redistribution, a problem that hasn't even been addressed sofar.

What about other chromospheric diagnostics? Hα is a yet nastier line, mixing large excitation sensitivity with large ionization sensitivity (Schoolman 1972), including complex recombination after photoionization in He I 10830 Å fashion. The TRACE near-UV images have lower resolution than the best Ca II K images (examples in Rutten et al. 1999), but even if they had, they suffer from similar photon diffusion because the solar ultraviolet bound-free continua are NLTE scatterers just like resonance lines (cf. lecture notes at `http://www.astro.uu.nl/~rutten`). Far-infrared imaging, beyond 160 μm, would do much better thanks to LTE formation but requires huge aperture to obtain the required resolution. Higher up, the Lyman sequence lines accessible to SUMER (Curdt & Heinzel 1998) may furnish the best diagnostics, although they are affected by multi-level photon conversion in Zanstra fashion.

What are fibrils/mottles/spicules?

What do fibrils/mottles/spicules do?

Why are fibrils/mottles/spicules so dark in TRACE 171 Å?

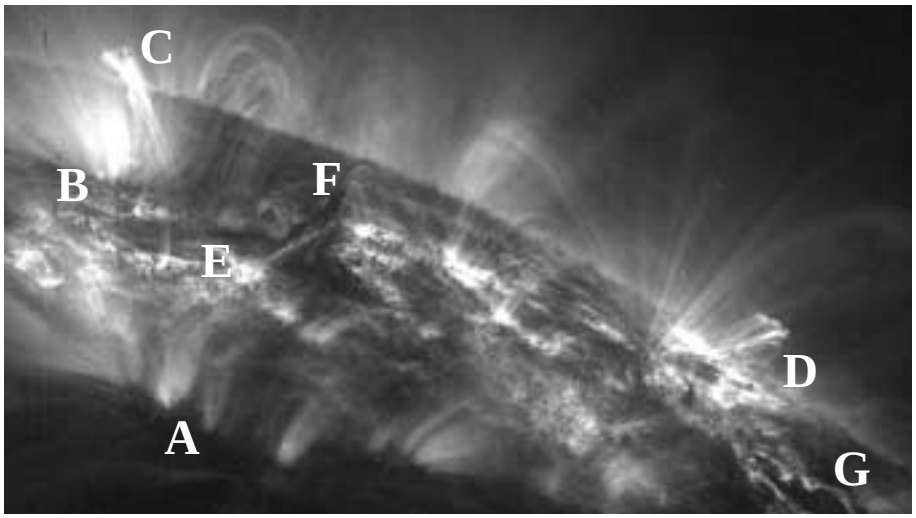

Figure 9. A TRACE 171 Å exposure copied from K&K. The Fe IX and Fe X emission lines in the passband portray gas at one million degrees and produce dramatic pictures because they pick out the relatively few loops at this temperature as if one sees only the aspen trees scattered through a thick but transparant pine tree forest of hotter loops. The latter appear only by causing the bright component of the low-lying "moss" seen near E and F and elsewhere, presumably through thermal conduction (Berger et al., in preparation). Most of the loops are optically thin, as evident near D where the emission scales with line-of-sight path length through the loop tops. The limb, the moss, and other areas also show fibrils in absorption. These are very opaque due to non-monochromatic bound-free scattering explained in Fig. 10. The other labeled features are described by K&K.

I lump these three questions together because I have an answer only to the third one. Spicules seem observationally ignored since the comprehensive review by Beckers (1968). Hα fibrils and mottles, schematically indicated in the K&K diagram in Fig. 3, also seem to await the completion of THEMIS, its MSDP spectrometer (Mein & Rayrole 1991), and development of diagnostics as the ones developed by Gontikakis et al. (1997) for prominences.

Theoretically, these features are all unexplained. An attractive suggestion by van Ballegooijen & Nisenson (1999) is that spicules appear in the separatrix layers (Van Ballegooijen et al. 1998) between neighboring fluxtubes sliding past each other as governed by footpoint migration, setting up strong shear flows.

TRACE 171 Å images show dark fibrils in great abundance, Figure 9 displays, amidst a host of intriguing structure, the presence of forests of dark absorption features that intercept the bright 10^6 K background. The absorption mechanism is likely to be similar to the longer-wavelength suggestion by Kucera et al. (1998) and is explained in Fig. 10. The bound-free extinction is probably dominated by scattering rather than thermal destruction. In contrast to the bound-bound scattering discussed for EUV lines by Mewe et al. (1995), such

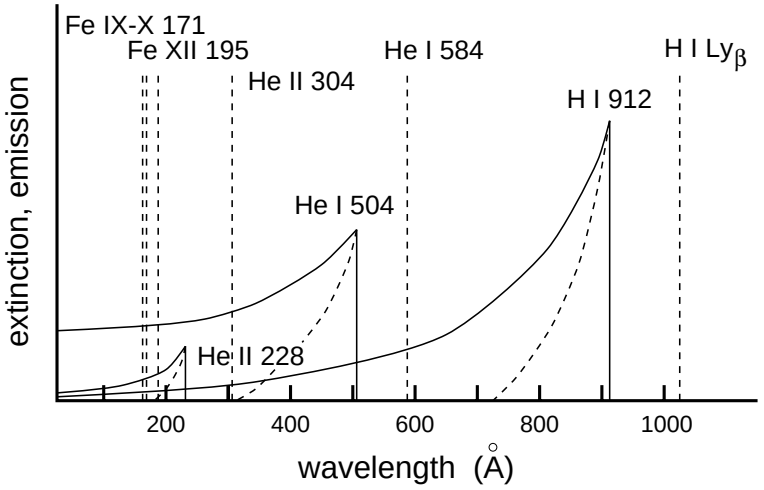

Figure 10. Schematic emission (dashed) and extinction (solid) variations with wavelength. Photons emitted by 10^6 K loops in the 171 Å lines may be extincted through H I, He I and He II photoionization in much cooler foreground material. In subsequent radiative recombination the photon will be re-emitted not only in another direction but also at another wavelength, near threshold. The actual extinction ratios depend on species ionization; at 171 Å hydrogen extinction dominates below $T \approx 8000$ K whereas He I dominates by two orders of magnitude at 10000 K but looses to He II extinction around 14000 K. The 195 Å line is similarly affected. Features that appear dark in these lines may appear dark or bright or disappear in He II 304 Å, He I 584 Å and the Lyman and Balmer H I lines.

bound-free scattering is not monochromatic because spontaneous recombination (the most likely process to follow radiative ionization) re-emits the absorbed photons preferentially near the ionization threshold. Each bound-free scattering sequence therefore not only redirects a 171 Å photon but also shifts it out of the TRACE bandpass. The observed darkness therefore does not measure temperature even for thick structures. However, the matter causing this extinction has to be sufficiently cool to contain fair amounts of at least He^+ but also neutral hydrogen when observable in Hα. The transition region is anything but shell-like in the moss regions of Fig. 9.

How is the network heated?

Finally the key network question. Wave heating has often been proposed but no wave modes have been identified. Figure 11 displays modulation power per pixel in various temporal frequency bands for a quiet disk-center area observed by TRACE. This mission gathers superb image sequences at high cadence without any seeing deformations. They are quite suited to Fourier analysis and permit to check characteristics of network oscillations that sofar have been diagnosed primarily from the wings of Hα (Kneer & von Uexküll 1983, 1985, 1986), the Ca II infrared lines (Deubner & Fleck 1989, 1990, Fleck & Deubner 1989), and

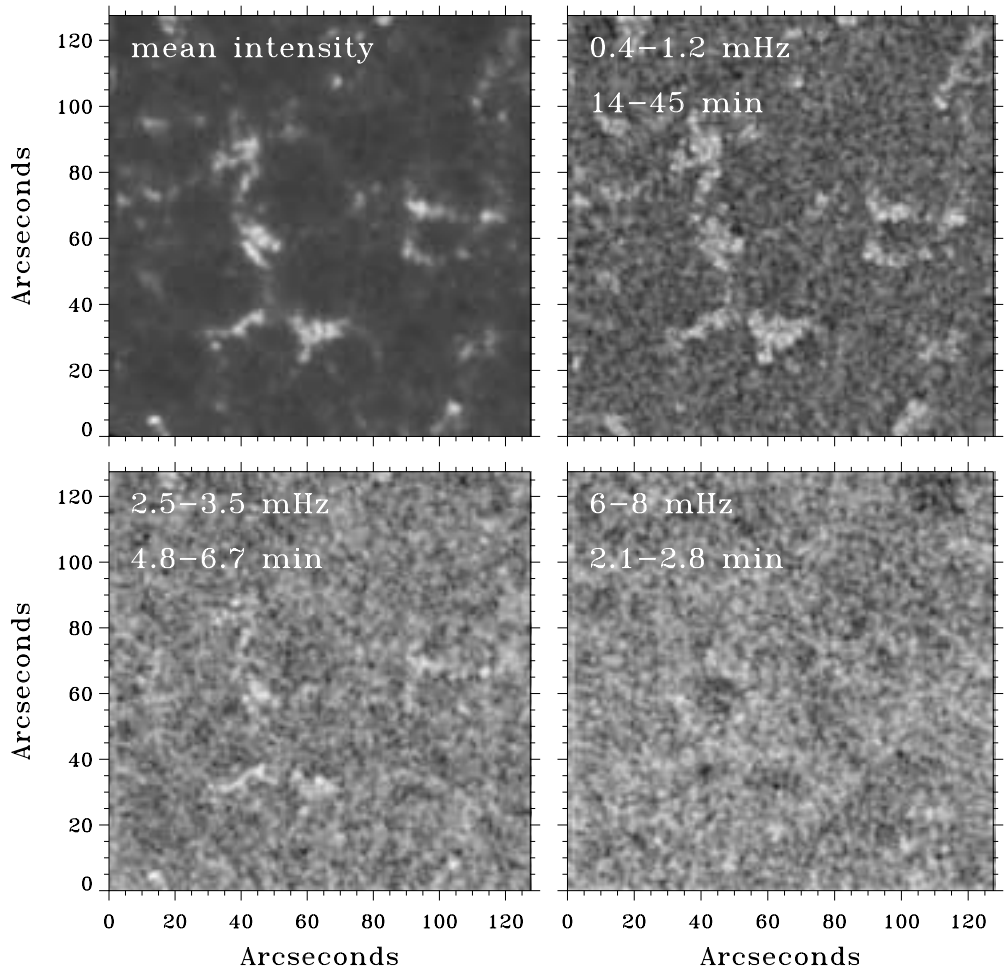

Figure 11. TRACE maps displaying Fourier power per pixel recorded in the 1700 Å channel on May 12, 1998 during UT 14:30–16:00 (JOP 72). The grey scale is logarithmic and has been readjusted for each panel separately. The first panel shows the temporally averaged linear intensity. The network (bright in first panel) has excess power at low frequency and power deficits with surrounding halos at high frequency. Data reduction bij J.M. Krijger.

Ca II H (Lites et al. 1993), with SUMER studies started (Judge et al. 1997, Curdt & Heinzel 1998). The general conclusion is that network shows no power of particular interest above $f = 3$ mHz, in contrast to internetwork regions which display enhanced power at higher frequencies especially in Dopplershift. This dichotomy is far from new, although it is often presented as such; it was already established by Jensen & Orrall (1963) and Liu & Sheeley (1971). The power maps in Fig. 11 demonstrate it once again.

What causes the low-frequency power displayed by the network? The highly dynamical nature of the filigree grains documented by e.g., Muller et al. (1989),

Muller & Roudier (1992) and Berger & Title (1996) certainly makes up a large part of it; perhaps the chromospheric power should all be attributed to footpoint motions as suggested by Kneer & von Uexküll (1985, 1986). Lites et al. (1993) thought to recognize wave signatures in Ca II H_3 Dopplershift time slices but from a small sample without spatial information from besides the stationary spectrometer slit. Kalkofen (1999, these proceedings) takes the rightmost peak in their Fig. 6 as significant and as evidence for tube waves — but that trust seems premature to his co-authors in the absence of larger data sets.

3. Internetwork issues

Are there weak internetwork fluxtubes?

The debate on the presence and properties of the elusive weak internetwork fields hasn't settled yet. It started with the surface-covering bipolar pepper-and-salt pattern of Livingston & Harvey (1971), deemed non-noise because its 2 arcsec single-polarity patches (with 5×10^{16} Mx or 2 Mx cm^{-2} apparent flux density, Harvey 1977) exceeded the magnetogram pixel size. The latest Sac Peak Fe I 1.56 μm Stokes spectrometry by Lin & Rimmele (1999) suggests instead that at the claimed 1 Mx cm^{-2} sensitivity much smaller flux concentrations appear in intergranular lanes that vary fast in response to the buffeting by surrounding granules. Lin & Rimmele (1999) estimate the flux per feature to be mostly below 5×10^{16} Mx and the intrinsic field strength mostly well below 500 Gauss, not peaking at 500 Gauss as claimed by Lin (1995).

The three isolated intergranular features marked in Fig. 6 behave just like these, vanishing intermittently in both diagnostics. They may mark temporary flux concentrations at the upper end of a turbulent spectrum that are yet too weak for convective collapse, or small-flux cousins to strong-field fluxtubes that underwent only weak collapse in which the convective collapse was hampered by sideways irradiation (Venkatakrishnan 1986), or shallow-rooted concentrations that didn't have sufficient collapse depth, or the remains of instability-split network tubes that became thin enough to be radiation-heated and weaken from convective blow-up in the reverse of the collapse process (Spruit 1979, Sect. 6.4.3 K&K). Discussions in the literature mostly concern the first two possibilities (e.g., Solanki et al. 1996) but the last one seems likely to me. This process should help to remove quiet network, a necessity to balance the intake from ephemeral regions.

However, isolated grains as the three in Fig. 6 are not as densely covering quiet internetwork lanes on high-resolution G-band images as the intergranular flux concentrations of Lin & Rimmele (1999) appear to do. I hope to see their results confirmed by infrared polarimetry with the new IAC TIP polarimeter at the German VTT (Collados 1999, these proceedings).

Are there identifiable shock pistons?

The explanation of Ca II H_{2V} and K_{2V} grain formation by internetwork shock interactions between upward propagating acoustic waves is now well established and therefore cartoonized in Fig. 2. A lingering debate is whether the internetwork grains (a better name since they are also seen in the TRACE near-UV

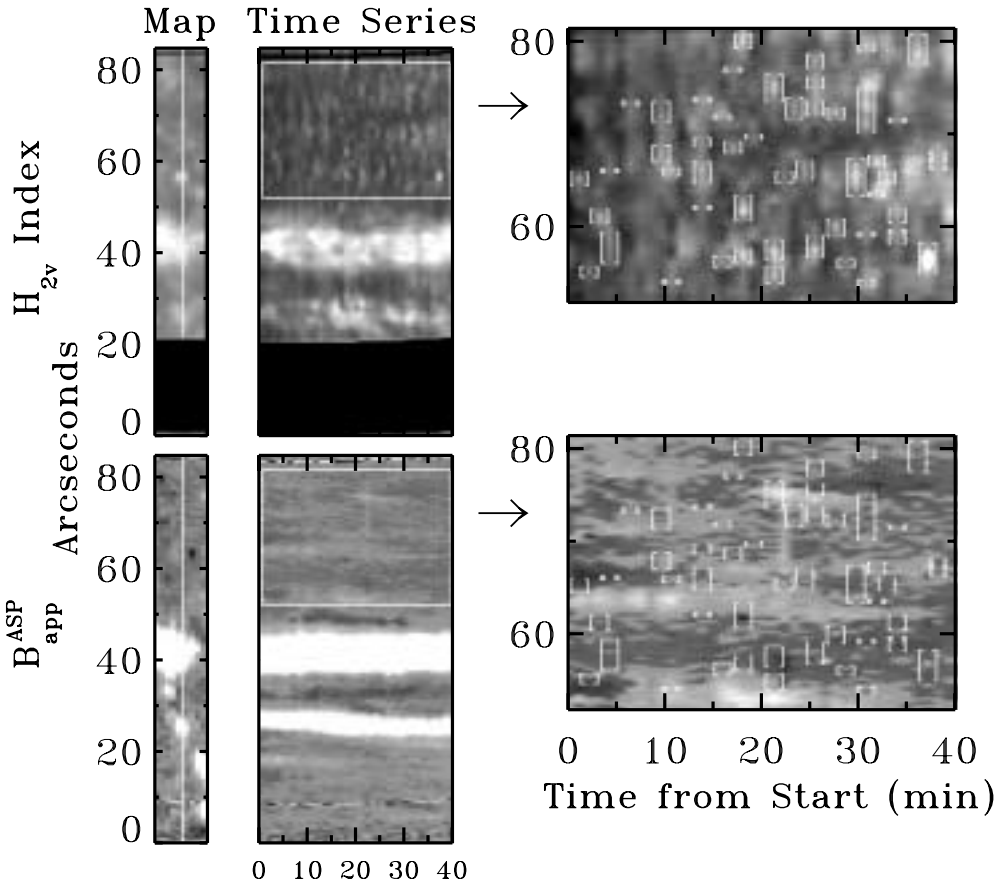

Figure 12. Comparison between Ca II H_{2V} brightness and apparent magnetic flux density measured with the Advanced Stokes Polarimeter at the Dunn Solar Telescope. The narrow panels at left are spatial maps of the two quantities build up by stepping the ASP slit sequentially over 11 arcsec. The white columns mark a selected slit position. A bright H_{2V} grain occurred near $y = 57''$ at this time. The two middle panels are space-time charts showing the time evolution of the two quantities along that slit position. There are network features around $y = 40''$ and $y = 27''$ of which the flux display is saturated in order to bring out weak fields. The H_{2V} brightness shows a characteristic three-minute modulation pattern; the bright grain in the spatial map occurred at $t = 37$ min. The superimposed box defines a quiet internetwork region for which the space-time charts are magnified at right. The brackets outline peak H_{2V} emission. There is no obvious correspondence to magnetic field features in the lower panel. From Lites et al. (1999).

channels, see Rutten et al. 1999) mark sites of enhanced magnetic field. Figure 12 shows that this is not the case at the 3 Mx cm^{-2} sensitivity level reliably reached

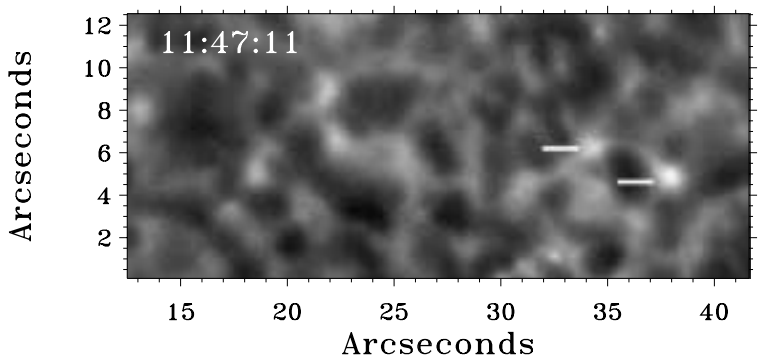

Figure 13. The wispy pattern seen in internetwork regions in Ca II K. The quietest region of the data sampled also in Fig. 6. Two K_{2V} grains (markers) brighten simultaneously, I bet due to a granular collapse event between them. From Lites et al. (1999) where this quiet area is also shown at subsequent moments.

with the ASP at Sac Peak. There is certainly no one-to-one grain-to-field correspondence as claimed by Sivaraman & Livingston (1982) and Sivaraman (1991). The same holds for the other ten chart pairs from these data, with the exception of one possible feature that behaves as the "persistent flashers" marked in Fig. 6.

I think it much more likely that the brighter internetwork grains betray hydrodynamical pistons, and have added these self-confidently to the paradigms of Fig. 2. The scenario is that downflows follow when the upflow is pulled out from under a small granule, and that the small-granule collapse excites waves excessively and leaves a dark "intergranular hole". The scenario comes from Mark Rast, the numerical simulation detailing it from Roar Skartlien in a recent Oslo thesis, and the scheme agrees with the event, hole and correspondence observations of Restaino et al. (1993), Rimmele et al. (1995), Roudier et al. (1997), Hoekzema et al. (1998a, 1998b), Hoekzema & Rutten (1998) and Goode et al. (1998). However, the definite identification must yet be made. Combination of TRACE white light and near-UV imagery provides probably a suitable way to try this. Whether it is feasible, even if there is a causal connection between granular collapse exciters and shocked internetwork grains, depends also on the amount of acoustic diffraction and the slant of the upward propagating waves (Fig. 11 of Hoekzema et al. 1998b).

How much heating from Ulmschneider's weak shocks?
Where is Ayres' COmosphere?
What constitutes Schrijver's basal flux?

These personalized questions are all answered in Fig. 14, at least schematically. I think it likely that the piston in the Carlsson-Stein (1997) simulation indeed didn't have the amount of high-frequency power that it should have had according to Ulmschneider (1999), because it was taken from the Dopplershifts of an iron line in the data of Lites et al. (1993) that did not faithfully follow fast motions. I buy Ulmschneider's suggestion that the time-averaged tempera-

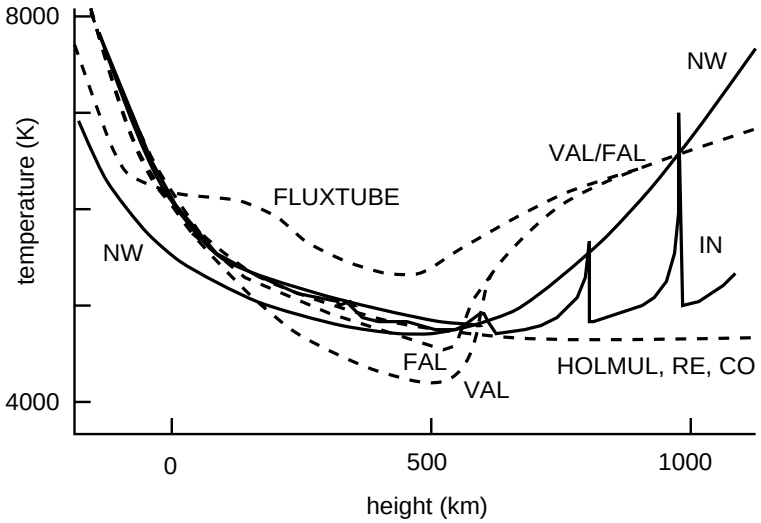

Figure 14. Schematic cartoon of solar model atmospheres. Dashed: standard models. VAL = Vernazza et al. (1981), FAL = Fontenla et al. (1993), HOLMUL = Holweger & Müller (1974), RE = radiative equilibrium, e.g., Bell et al. (1976), CO = a model based on CO line brightness temperatures yet to be constructed, FLUXTUBE = a 1.5D fluxtube model such as from Briand & Solanki (1995). Solid: "Rotten conjectures" for the internetwork (IN) and network (NW), respectively a sample of the instantaneous temperature in the internetwork (IN) and the average temperature in a magnetic element cluster (NW).

ture should go up somewhere around $h = 800 - 1000$ km due to high-frequency dissipation. Until that height, the CO line core brightnesses should faithfully show the time-averaged internetwork temperature because the CO dissociation equilibrium is too slow to be much disrupted by passing shocks. That explains Ayres' COmosphere (e.g., Wiedemann et al. 1994) but is difficult to simulate numerically because time-dependent molecule formation in shocks isn't easy. Schrijver's (1992) basal flux *must* arise acoustically since there isn't anything ubiquitously present in internetwork areas at Ca II K formation height other than the wispy patterns exemplified in Fig. 13. The K_{2V} grains are local enhancements of this pattern but it all contributes. Its wave nature is immediately obvious when sequences of such images are played as video movies. You might try that yourself with a TRACE UV sequence, for example the ones taken in JOP72 on May 12, 1998 (cf. Fig. 11).

Acknowledgements. I thank the organizers for an excellent workshop, for inviting me to give this review, and for their leniency in deadline coercion. Various items above gained content from discussions before, during and after the meeting, in particular with J.M. Beckers, T.E. Berger, M. Cuntz, B.W. Lites, J. Sánchez Almeida, C.J. Schrijver, O. Steiner, P. Ulmschneider and C. Zwaan, and from access to the manuscript and figure files of Schrijver & Zwaan (1999). Although this meeting was a European one, some of the new material displayed here comes from the US TRACE mission thanks to its commendable open data policy and easy web access which I acknowledge gratefully.

This work is part of the EC–TMR European Solar Magnetometry Network (ESMN). Studying G-band formation is supported by NASA SR&T Grant NASW–98008.

References

Auffret H., Muller R., 1991, A&A 246, 264
Beckers J. M., 1968, Solar Phys. 3, 367
Beckers J. M., 1976, in D. J. Williams (ed.), Procs. Int. Symp. Solar–Terrestrial Phys., Am. Geophys. Union, p. 89
Bell R. A., Eriksson K., Gustafsson B., Nordlund Å., 1976, A&AS 23, 37
Berger T. E., Löfdahl M. G., Shine R. A., Title A. M., 1998a, ApJ 506, 439
Berger T. E., Löfdahl M. G., Shine R. S., Title A. M., 1998b, ApJ 495, 973
Berger T. E., Schrijver C. J., Shine R. A., Tarbell T. D., Title A. M., Scharmer G., 1995, ApJ 454, 531
Berger T. E., Title A. M., 1996, ApJ 463, 365
Briand C., Solanki S., 1995, A&A 299, 596
Bünte M., Solanki S. K., Steiner O., 1993, A&A 268, 736
Carlsson M., Rutten R. J., Shchukina N. G., 1992, A&A 253, 567
Carlsson M., Stein R. F., 1994, in M. Carlsson (ed.), Chromospheric Dynamics, Proc. Miniworkshop, Inst. Theor. Astrophys., Oslo, p. 47
Carlsson M., Stein R. F., 1995, ApJ 440, L29
Carlsson M., Stein R. F., 1997, ApJ 481, 500
Carlsson M., Stein R. F., 1999, in B. Schmieder, A. Hofmann, J. Staude (eds.), Solar Magnetic Fields and Oscillations, Procs. Third Adv. Solar Physics Euroconf., Astron. Soc. Pac. Conf. Series, in press
Collados M., 1999, in B. Schmieder, A. Hofmann, J. Staude (eds.), Solar Magnetic Fields and Oscillations, Procs. Third Adv. Solar Physics Euroconf., Astron. Soc. Pac. Conf. Series, in press
Curdt W., Heinzel P., 1998, ApJ 503, L95
Deubner F.-L., Fleck B., 1989, A&A 213, 423
Deubner F.-L., Fleck B., 1990, A&A 228, 506
Dunn R. B., Zirker J. B., 1973, Solar Phys. 33, 281
Fleck B., Deubner F.-L., 1989, A&A 224, 245
Fontenla J. M., Avrett E. H., Loeser R., 1993, ApJ 406, 319
Foukal P., 1990, Solar Astrophysics, Wiley and Sons, New York
Fraunhofer J., 1817, Denkschriften der Münch. Akad. der Wissenschaften 5, 193
Giovanelli R. G., 1980, Solar Phys. 68, 49
Golub L., Krieger A. S., Silk J. K., Timothy A. F., Vaiana G. S., 1974, ApJ 189, L93
Gontikakis C., Vial J. C., Gouttebroze P., 1997, A&A 325, 803
Goode P. R., Strous L. H., Rimmele T. R., Stebbins R. T., 1998, ApJ 495, L27
Harvey J., 1977, Highlights of Astronomy 4 Part II, 223
Harvey K. L., Martin S. F., 1973, Solar Phys. 32, 389
Hoekzema N. M., Brandt P. N., Rutten R. J., 1998a, A&A 333, 322
Hoekzema N. M., Rutten R. J., 1998, A&A 329, 725
Hoekzema N. M., Rutten R. J., Brandt P. N., Shine R. A., 1998b, A&A 329, 276
Hoekzema N. M., Rutten R. J., Cook J. W., 1997, ApJ 474, 518
Holweger H., Müller E. A., 1974, Solar Phys. 39, 19
Jensen E., Orrall F. Q., 1963, PASP 75, 162
Judge P., Carlsson M., Wilhelm K., 1997, ApJ 490, L195
Kalkofen W., 1999, in B. Schmieder, A. Hofmann, J. Staude (eds.), Solar Magnetic Fields and Oscillations, Procs. Third Adv. Solar Physics Euroconf., Astron. Soc. Pac. Conf. Series, in press

Keller C. U., Deubner F.-L., Egger U., Fleck B., Povel H. P., 1994, A&A 286, 626
Kneer F., 1981, A&A 93, 387
Kneer F., von Uexküll M., 1983, A&A 119, 124
Kneer F., von Uexküll M., 1985, A&A 144, 443
Kneer F., von Uexküll M., 1986, A&A 155, 178
Kucera T. A., Andretta V., Poland A. I., 1998, Solar Phys. 183, 107
Lin H., 1995, ApJ 446, 421
Lin H., Rimmele T., 1999, ApJ 514, in press
Lites B. W., Leka K. D., Skumanich A., Martínez Pillet V., Shimizu T., 1996, ApJ 460, 1019
Lites B. W., Rutten R. J., Berger T. E., 1999, ApJ 517, , in press
Lites B. W., Rutten R. J., Kalkofen W., 1993, ApJ 414, 345
Liu S. Y., Sheeley N. R., 1971, Solar Phys. 20, 282
Livi S. H. B., Wang J., Martin S. F., 1985, Australian Journal of Physics 38, 855
Livingston W., Harvey J., 1971, in R. Howard (ed.), Solar Magnetic Fields, IAU Symposium 43, Reidel, Dordrecht, p. 51
Löfdahl M. G., Berger T. E., Shine R. S., Title A. M., 1998, ApJ 495, 965
Martin S. F., 1988, Solar Phys. 117, 243
Mein P., Rayrole J., 1991, Advances in Space Research 11, 151
Mewe R., Kaastra J. S., Schrijver C. J., Van Den Oord G. H. J., Alkemade F. J. M., 1995, A&A 296, 477
Mount G. H., 1975, Ph.D. thesis, Colorado Univ., Boulder.
Muller R., 1994, in R. J. Rutten, C. J. Schrijver (eds.), Solar Surface Magnetism, NATO ASI Series C Vol. 433, Kluwer, Dordrecht, p. 55
Muller R., Dollfus A., Montagne M., Moity J., Vigneau J., 1999, in B. Schmieder, A. Hofmann, J. Staude (eds.), Solar Magnetic Fields and Oscillations, Procs. Third Adv. Solar Physics Euroconf., Astron. Soc. Pac. Conf. Series, in press
Muller R., Hulot J. C., Roudier T., 1989, Solar Phys. 119, 229
Muller R., Roudier T., 1992, Solar Phys. 141, 27
Rast M. P., 1995, ApJ 443, 863
Rast M. P., 1999a, ApJ submitted
Rast M. P., 1999b, in T. Rimmele, K. Balasubramaniam, R. Radick (eds.), High Resolution Solar Physics: Theory, Observations, and Techniques, Procs. 19th NSO/Sacramento Peak Summer Workshop, Astron. Soc. Pac. Conf. Series, in press
Reeves E. M., 1976, Solar Phys. 46, 53
Restaino S. R., Stebbins R. T., Goode P. R., 1993, ApJ 408, L57
Rimmele T. R., Goode P. R., Harold E., Stebbins R. T., 1995, ApJ 444, L119
Roudier T., Espagnet O., Muller R., Vigneau J., 1994, A&A 287, 982
Roudier T., Malherbe J. M., November L., Vigneau J., Coupinot G., Lafon M., Muller R., 1997, A&A 320, 605
Rutten R. J., 1995, in J. T. Hoeksema, V. Domingo, B. Fleck, B. Battrick (eds.), Helioseismology, Proc. Fourth SOHO Workshop, ESA SP–376 Vol. 1, ESA Publ. Div., ESTEC, Noordwijk, p. 151
Rutten R. J., 1998, in C. Fröhlich, M. C. E. Huber, S. Solanki, R. von Steiger (eds.), Solar Composition and its Evolution – from Core to Corona, Procs. ISSI Workshop, Space Sci. Rev. 85, p. 269
Rutten R. J., Carlsson M., 1994, in D. M. Rabin, J. T. Jefferies, C. Lindsey (eds.), Infrared Solar Physics, Proc. Symp. 154 IAU (Tucson), Kluwer, Dordrecht, p. 309
Rutten R. J., de Pontieu B., Lites B. W., 1999, in T. Rimmele, K. Balasubramaniam, R. Radick (eds.), High Resolution Solar Physics: Theory, Observations, and Techniques, Procs. 19th NSO/Sacramento Peak Summer Workshop, Astron. Soc. Pac. Conf. Series, in press

Rutten R. J., Uitenbroek H., 1991, Solar Phys. 134, 15
Schoolman S. A., 1972, Solar Phys. 22, 344
Schrijver C. J., 1992, A&A 258, 507
Schrijver C. J., Title A. M., Harvey K. L., Sheeley N. R., Wang Y.-M., van den Oord G. H. J., Shine R. A., Tarbell T. D., Hurlburt N. E., 1998, Nat 394, 152
Schrijver C. J., Title A. M., Van Ballegooijen A. A., Hagenaar H. J., Shine R. A., 1997, ApJ 487, 424
Schrijver C. J., Zwaan C., 1999, Solar and Stellar Magnetic Activity, Cambridge Univ. Press, in press (K&K)
Simon G. W., Zirker J. B., 1974, Solar Phys. 35, 331
Sivaraman K. R., 1991, in P. Ulmschneider, E. Priest, B. Rosner (eds.), Mechanisms of Chromospheric and Coronal Heating, Heidelberg Conference, Springer Verlag, Berlin, p. 44
Sivaraman K. R., Livingston W. C., 1982, Solar Phys. 80, 227
Skartlien R., 1998, 3D modeling of solar convection and atmosphere dynamics, PhD thesis, Inst. Theor. Astrophys. Oslo
Solanki S., Steiner O., Uitenbroek H., 1991, A&A 250, 220
Solanki S., Zufferey D., Lin H., Rüedi I., Kuhn J., 1996, A&A 310, L33
Spruit H. C., 1976, Solar Phys. 50, 269
Spruit H. C., 1977, Magnetic flux tubes and transport of heat in the convection zone of the Sun, PhD thesis, Utrecht University
Spruit H. C., 1979, Solar Phys. 61, 363
Spruit H. C., Title A. M., Van Ballegooijen A. A., 1987, Solar Phys. 110, 115
Spruit H. C., Zwaan C., 1981, Solar Phys. 70, 207
Stein R. F., Nordlund Å., 1989, ApJ 342, L95
Steiner O., 1999, in B. Schmieder, A. Hofmann, J. Staude (eds.), Solar Magnetic Fields and Oscillations, Procs. Third Adv. Solar Physics Euroconf., Astron. Soc. Pac. Conf. Series, in press
Steiner O., Grossmann-Dörth U., Knölker M., Schüssler M., 1998, ApJ 495, 468
Stenflo J. O., Harvey J. W., 1985, Solar Phys. 95, 99
Stix M., 1989, The Sun. An Introduction, Springer, Berlin
Title A. M., Berger T. E., 1996, ApJ 463, 797
Ulmschneider P., 1999, in C. Butler, J. Doyle (eds.), Solar and Stellar Activity: Similarities and Differences, Procs. Armagh Workshop, Astron. Soc. Pac. Conf. Series, in press
van Ballegooijen A., 1985, in H. U. Schmidt (ed.), Theoretical Problems in High Resolution Solar Physics, Procs. Solar Opt. Tel. Workshop, Max Planck Inst. Astrophysik, München, 177
van Ballegooijen A. A., Nisenson P., 1999, in T. Rimmele, K. Balasubramaniam, R. Radick (eds.), High Resolution Solar Physics: Theory, Observations, and Techniques, Procs. 19th NSO/Sacramento Peak Summer Workshop, Astron. Soc. Pac. Conf. Series, in press
Van Ballegooijen A. A., Nisenson P., Noyes R. W., Löfdahl M. G., Stein R. F., Nordlund Å., Krishnakumar V., 1998, ApJ 509, 435
Venkatakrishnan P., 1986, Nat 322, 156
Vernazza J. E., Avrett E. H., Loeser R., 1981, ApJS 45, 635
Wang J., Zhang J., 1999, in B. Schmieder, A. Hofmann, J. Staude (eds.), Solar Magnetic Fields and Oscillations, Procs. Third Adv. Solar Physics Euroconf., Astron. Soc. Pac. Conf. Series, in press
Wiedemann G., Ayres T. R., Jennings D. E., Saar S. H., 1994, ApJ 423, 806
Zwaan C., Cram L. E., 1989, in L. E. Cram, L. V. Kuhi (eds.), FGK Stars and T Tauri Stars, Monogr. series nonthermal phenomena in stellar atmospheres, CNRS–NASA, US Govt. Printing Office, p. 215